Prediction of a strain-induced conduction-band minimum in embedded quantum dots

A. J. Williamson and Alex Zunger
National Renewable Energy Laboratory, Golden, Colorado 80401

A. Canning
NERSC, Lawrence Berkeley National Laboratory, Berkeley, California 94720
~Received 17 November 1997!

Free-standing InP quantum dots have previously been theoretically and experimentally shown to have a direct band gap across a large range of experimentally accessible sizes. We demonstrated that when these dots are embedded coherently within a GaP barrier material, the effects of quantum confinement in conjunction with coherent strain suggest there will be a critical diameter of dot ~ ' 60 Å!, above which the dot is direct, type I,

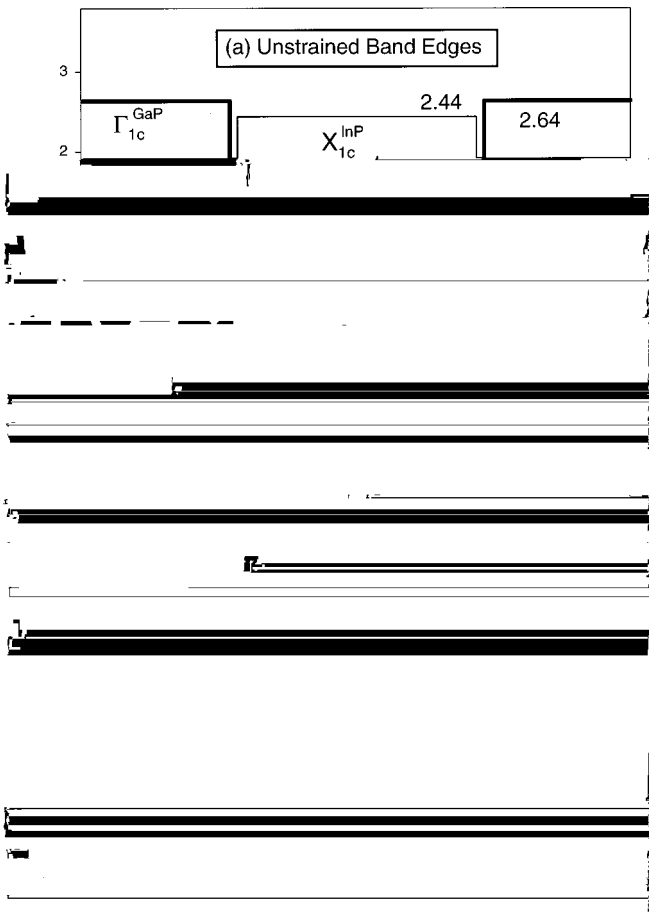

FIG. 1. ~a! Unstrained ~''natural''! band offsets ~in eV! between bulk GaP and InP. Solid lines indicate bulk band edges and dashed lines indicate quantum confined levels. Arrows show the energy change due to confinement. G-derived states are shown with thick lines and *X*-derived states with thin lines. ~b! Strain-modified band edges $E_{nk}@e(\mathbf{R})\#$ are plotted along @100# through the center of the InP dot with diameter 131 Å and dot-dot separation of 109 Å. The lowest ~highest! conduction ~valence! band is shown at each position **R**. The * denotes the position at which the lowest conduction state is localized.

separation is large enough to remove any dot-dot interactions. However, in the systems studied here, the large barrier sizes create such a high GaP:InP ratio ~ ; 30:1! that any external relaxation would be minimal in any case. The resulting strain exhibits nontrivial hydrostatic and biaxial components. Our quantum-mechanical calculation of the energy levels of the dot ~see below! will include the effect of such a strain profile. However, in order to understand these results, we first consider a simpler case, namely we calculate the band-edge states of *bulk* InP and *bulk* GaP subject to the local strain $e(\mathbf{R})$ experienced by the GaP-embedded InP dot at position **R**. To do this we discretize the GaP/InP nanostructure into ''cells'' with position vector **R** and then perform ; 40 bulk band-structure calculations of InP and GaP, using the empirical pseudopotential method,[11] thus obtaining the bulk eigenvalues $E_{nk}@e(\mathbf{R})\#$ for band *n* at wave vector *k* within each cell. Each bulk calculation $E_{nk}@e(\mathbf{R})\#$ uses the In-P or Ga-P bond geometry within that cell. The resulting strain-modified band-edge states are shown in Fig. 1~b!. Compared with the unstrained offsets @Fig. 1~a!#, we see that the GaP X_{1c} band edge that is flat in the absence of strain @Fig. 1~a!# is now transformed into an attractive trough @indicated by * in Fig. 1~b!#, capable of localizing electrons. The formation of this trough is initially surprising as the deformation potential at the X_{1c} point is negative and one might therefore expect the hydrostatic expansion of the GaP at the interface with the InP dot to drive the X_{1c} state up in energy. However, the above bulk calculations show that it is the *biaxial* strain present at this interface which is the dominant term, and this is capable of forming the electron troughs. The *atomistic* strain has therefore profoundly modified the nature of the confined electron states from delocalized to localized. It is important to emphasize that conventional[12] calculations of strain-modified conduction-band offsets include only the hydrostatic ~no biaxial! term and only the Γ_{1c} ~no X_{1c}) conduction band, and would therefore miss the important changes in the conduction-band edges between Figs. 1~a! and 1~b!, which our calculations show are due to the effect of biaxial deformation on the X_{1c} state.

Results of calculations on dots. To calculate the energy levels of GaP-embedded InP dots, we again place an InP dot of radius *R*, surrounded by sufficiently thick GaP barrier in a ''supercell,'' repeated periodically to create a lattice of dots. Having created ~artificial! translational periodicity, band theoretical models can then be applied to study the electronic properties. The limit of an isolated dot is achieved by increasing the thickness of the GaP barrier. The calculations for both the bulk bands and the quantum dot levels are based on the atomistic Hamiltonian

$$\hat{H} = -\tfrac{1}{2}\nabla^2 + \sum_{a,n} v_a(\mathbf{r} - \mathbf{R}_{an}). \qquad (1)$$

The total potential is constructed from screened atomic pseudopotentials, v_a, where *a* represents Ga, In, and P, and $\mathbf{R}_{an}$ are the relaxed atomic positions. The pseudopotentials v_a have been fitted[9] to the experimental band gaps, deformation potentials, and effective masses. We use the analytic form of the pseudopotential described in Ref. 9, which was designed to build in the effects of strain experienced by each atom in lattice mismatched systems.

The supercells studied in this paper contain up to one million atoms, which is too large for the Hamiltonian in Eq. (1) to be solved by direct diagonalization. We thus use the folded spectrum method[13,14] (FSM), in which one solves for the eigenstates of the equation

$$(\hat{H} - e_{\mathrm{ref}})^2 c_i = (e - e_{\mathrm{ref}})^2 c_i, \qquad (2)$$

where e_{ref} is a reference energy, and the wave functions c_i are expanded in a plane-wave basis. By placing e_{ref} within the gap, and close to the valence-band maximum or conduction-band minimum (CBM), one is then able to obtain the top few valence states or the bottom few conduction states, respectively. Using this approach the computational cost scales as $MN\ln(N)$, where *N* is the number of desired electronic states and *M* is the number of plane-wave basis functions (M ' 20 million in the largest system studied here!. The simulations in this paper were performed using a parallel code on the Cray T3E900 on up to 256 processors where the

ellipsoid of **g** vectors is divided over the processors in a similar way to the method used by Clarke, Stich, and Payne.[15] Using this data distribution and fast parallel fast Fourier transforms almost linear speedup with the number of processors can be obtained for the large systems studied.

To facilitate comparison with the spherical freestanding InP quantum dots studied in Ref. 4, we constructed a series of supercells containing spherical InP quantum dots with diameters of 44, 87, 131, and 174 Å. Each dot was surrounded with sufficient GaP barrier material to produce dot-dot separations of 109, 152, 196, and 239 Å, respectively. The calculated energies of the highest occupied valence states and lowest empty conduction states are shown in Fig. 2. The left-hand side of Fig. 3 illustrates the corresponding wave functions squared of the 131-Å dot. We see that the highest-energy valence wave function is localized within the InP dot @Fig. 3~c!#, whereas the lowest conduction wave function is localized in pockets at the $001% facets of the interface between the InP dot and the GaP barrier @Fig. 3~b!#. The energy of this interfacial state is considerably lower than the unstrained bulk GaP X_{1c} state ~solid horizontal line in Fig. 2! for all the dots studied. To establish the identify of these wave functions in terms of the parent GaP and InP bulk states, we project the dot wave functions c_i into the zinc-blende Brillouin zone using the method described in Ref. 16.

in each of the four InP quantum dots are shown in Fig. 2. Figure 2 shows that there is a critical dot diameter around 60 Å below which the G_{1c}-derived conduction state in the InP quantum dot is higher in energy than the bulk X_{1c} state of the GaP barrier. This is a type I to type II transition. However, for all sizes of InP dot, the G_{1c}-derived state is higher in energy than the X_{1c}-like interfacial state.

In conclusion, we have shown that ~i! the effects of quantum confinement and pressure raise the energy of the G_{1c}-derived state in an InP quantum dot so that for dots smaller than 60 Å, this state is higher than the X_{1c} state of the unstrained GaP barrier. This transition is analogous to the AlAs-embedded GaAs dot, where the CBM moves from GaAs-G_{1c} to AlAs-X_{1c} as the GaAs size decreases. However, ~ii! strain induces an even lower energy state, indirect in reciprocal space and localized in real space at the interface between the InP dot and the GaP barrier. Therefore, we predict that even for large, spherical InP dots, as long as coherency is maintained, the effects of strain create a system with an indirect band gap that is considerably reduced due to the low-lying interfacial state. This is in direct contrast to the behavior of freestanding InP dots, which are direct over the large range of experimentally accessible sizes.

This work was supported by the United States Department of Energy-Basic Energy Services, Division of Materials Science, under Contract No. DE-AC36-83CH10093. The calculations were performed using the Cray T3E, located at the National Energy Research Scientific Computing Center, which is supported by the Office of Energy Research of the U.S. Department of Energy.

[1] O. Micic, C. Curtis, K. Jones, J. Sprague, and A. Nozik, J. Phys. Chem. **98**, 4966 ~1994!.

[2] N. Carlsson, W. Seifert, A. Petersson, P. Castrillo, M. Pistol, and L. Samuelson, Appl. Phys. Lett. **66**, 3093 ~1994!.

[3] C. Ulrich, S. Ves, A. Goni, A. Kurtenbach, K. Syassen, and K. Eberl, Phys. Rev. B **52**, 12 212 ~1995!.

[4] H. Fu and A. Zunger, Phys. Rev. B **55**, 1642 ~1997!; **56**, 1496 ~1997!.

[5] A. Franceshetti and A. Zunger, Appl. Phys. Lett. **68**, 3455 ~1996!.

[6] *Numerical Data and Functional Relationships in Science and Technology*, edited by O. Madelung, Landolt-Börnstein, New Series, Vol. 22, Pt. a ~Springer-Verlag, Berlin, 1997!.

[7] A. Franceshetti, S.-H. Wei, and A. Zunger, Phys. Rev. B **50**, R8094 ~1994!.

[8]